

## CHAPTER 4

*Kinetics and thermochemistry of hydrolysis mechanism of a novel anticancer agent trans-[PtCl<sub>2</sub>(dimethylamine)(isopropylamine)]:  
A DFT study*

---

### IN THIS CHAPTER-

- INTRODUCTION
- COMPUTATIONAL DETAILS
- STRUCTURAL ANALYSIS
- ENERGY PROFILES

### OUTLOOK-

- ✓ Detailed theoretical investigation has been performed on the two step hydrolysis mechanism of a novel transplatin anticancer agent *trans*-[PtCl<sub>2</sub>(dimethylamine)(isopropylamine)] in both gas as well as in aqueous phase using density functional theory (DFT).
- ✓ The existence of transition states on the corresponding PES is ascertained by performing intrinsic reaction coordinate calculations (IRC).
- ✓ The first hydrolysis step has found to have a faster compared to that of the second step, indicating the monoquo species of the complex is the most preferable species that react with the cellular DNA *in vivo*.
- ✓ The calculated rate constant also signifies that the second step hydrolysis is the rate-limiting process.

#### **4.1 Introduction**

The awareness of platinum-based antitumor drugs has its origin in 1960s, with the serendipitous Rosenberg's discovery of cell inhibition by Pt electrodes.<sup>1,2</sup> Cisplatin (*cis*-[PtCl<sub>2</sub>(NH<sub>3</sub>)<sub>2</sub>], *cis*-DDP) is one of the most extensively used anticancer drugs and is effective against ovarian, testicular, head and neck malignancies.<sup>3,4</sup> However, this antitumor agent exhibits some important dose-limiting toxicities, mainly nephrotoxicity, neurotoxicity, and ototoxicity.<sup>5,6</sup> There is not a single platinum based drug which is efficient against all cancer types and some cancer cells are also found to be inherently resistant to such clinically approved platinum chemotherapeutic agents. In addition, cancer cells can also acquire resistance over time by the process of somatic evolution.<sup>7</sup> In order to circumvent these issues, in the last thirty years, many investigations have been directed towards platinum based compounds endowed with higher anticancer activity and lower toxic effects than *cis*-DDP. In this search of novel *cis*-platin anticancer agents, certain *trans*-platin analogues are showing higher activity both *in vitro* and *in vivo* compared to their parent *cis*-isomers.<sup>8</sup>

Most of the structure/activity paradigm emerged from the initial studies by Cleare<sup>9,10</sup> and Hoeschele<sup>10</sup> have now been interrogated. It has been believed that the *trans*-analogues of cisplatin and monodentate charged complexes are therapeutically inactive.<sup>11</sup> The recent development of new highly active platinum based drugs do not coincide with the classical structure-activity rules; indicating the need for a re-evaluation of these rules. It has been noticed that there are certain transplatin complexes which are showing higher antitumor activity both *in vitro* as well as *in vivo*.<sup>12,13</sup> Thus, in the recent years these types of complexes are gaining much interest in the field of anticancer drug discovery.<sup>14</sup>

Farrel et al.<sup>15</sup> for the first time reported that there are certain transplatin complexes having planner amino ligands showing activity superior to cisplatin, especially in case of cisplatin resistant cell lines. The activity of such complexes could be increased by using bulky carrier ligands which reduces the rate of replacement of the chloro ligands. The bulky ligand would limit the axial access of the Pt-atom thereby inhibit the formation of five coordinated intermediate.<sup>16</sup> Examples of these antitumor trans-platinum complexes

are the analogues of transplatin in which one ammine group is replaced by ligands such as thiazole, piperidine, piperazine, 4-picoline and cyclohexylamine; the analogs with branched asymmetric aliphatic amines.<sup>17</sup>

It has been well established that the hydrolysis is the key activation step before reacting with its intercellular target DNA inside the cell.<sup>18-20</sup> Thus, considerable attention has been paid in recent years to perform experimental and theoretical studies on the hydrolysis of the platinum based complexes.<sup>21-28</sup> The cellular target of platinum based anticancer drugs are N7 atom of the purine bases *i.e.* guanine (G) and adenine (A) in the cellular DNA. It will first produce monofunctional adduct, which subsequently coordinates to N7 atom of another purine base generating bifunctional adducts through intrastrand and interstrand cross-links (CLs). Cisplatin adducts in linear DNA include 90% 1,2-d(GpG) or d(ApG) CLs with other lesions including 1,3-d(GpNpG) intrastrand CLs and to a lesser extent interstrand cross-links (ICLs), monofunctional adducts and various DNA protein CLs.<sup>29</sup> However, transplatinum complexes cannot form such intrastrand cross-links instead it will exhibit only monofunctional adducts, 1,3-intrastrand CLs and ICLs.<sup>30</sup> Thus, they will form a kinetically stable Pt-DNA adduct which is generally responsible for biological activity of such complexes.<sup>31</sup>

The first representative of this novel class of *trans*-platinum complexes is *trans*-[PtCl<sub>2</sub>(dimethylamine)(isopropylamine)], represented in Figure 4.1. The compound is a mixture of aliphatic amines, showing marked activity against *cis*-DDP resistance in Pam212-*ras* tumor cells and can induce cell death through apoptosis.<sup>32</sup> It was initially characterized by elemental analysis, mass spectrum, IR and NMR spectroscopic techniques.<sup>33</sup> The hydrolysis mechanism of this complex is studied here, which is characterized by an exchange of two ligands (the chlorine anion and the water molecule) and it belongs to the class of second-order nucleophilic substitution (S<sub>N</sub>2) reactions.

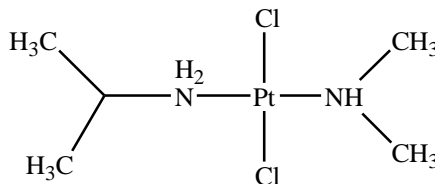
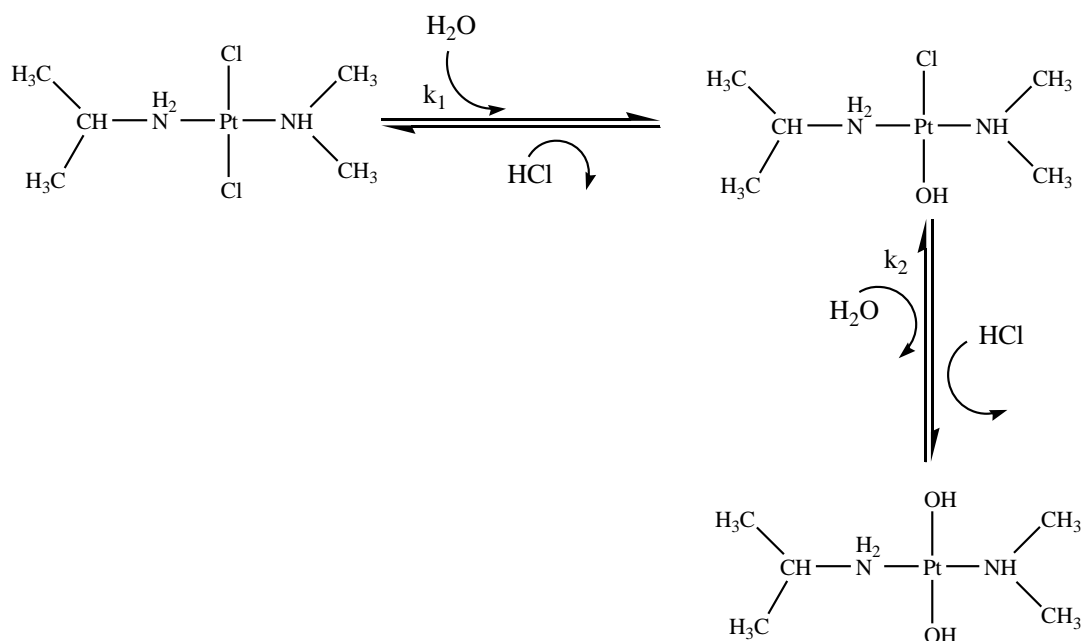


**Figure 4.1** Structural formula of *trans*-[PtCl<sub>2</sub>(dimethylamine)(isopropylamine)]

In this chapter, computational studies have been performed to explore the kinetics and mechanistic hydrolysis pathways of the novel transplatin anticancer agent *trans*-[PtCl<sub>2</sub>(dimethylamine)(isopropylamine)] according to the Scheme 4.1. Since, experimental studies can only provide the total rate constant value, it is quite inadequate in predicting the mechanism as well as the thermochemistry of a given reaction. Therefore, in order to get the detailed insight into mechanism, kinetics as well as thermochemistry, we must rely on the quantum chemical methods. To the best of our knowledge, this is the first theoretical report exploring the two step hydrolysis mechanism of this complex.



**Scheme 4.1** Reaction steps in *trans*-[PtCl<sub>2</sub>(dimethylamine)(isopropylamine)] hydrolysis

## 4.2 Computational Details

Geometry optimization of the species involved in the two step hydrolysis mechanism of a novel transplatin anticancer agent *trans*-[PtCl<sub>2</sub>(dimethylamine)(isopropylamine)] are made at density functional B3LYP<sup>34,35</sup> level of theory. During geometry optimization, 6-311G(d,p) basis set<sup>36</sup> is used for all elements except Pt. Considering the strong relativistic effect of Pt-atom, we have employed Los Alamos LanL2DZ basis set with effective core potential<sup>37</sup> for platinum atom only. In order to determine the nature of different stationary points on the potential energy surface (PES),

vibrational frequencies calculations are performed using the same level of theory at which the optimization are made. To obtained accurate hydrolysis picture of the complex, computational procedure are followed using aqueous phase polarized continuum-model (CPCM) also.<sup>38,39</sup>

In this investigation, we have considered minimal number of essential water molecule (only one explicit water molecule in our case) to reproduce the main features involved in the hydrolysis mechanism.<sup>40</sup> The prime objective of this study is to concentrate mainly on the hydrolysis process. Since, only one water molecule at a time is being utilized for the hydrolysis pathway, replacing the Cl<sup>-</sup> ion, we have used a single water solvent molecule for this study. Considering more water molecules into the system is not going to affect the overall mechanism of the hydrolysis.<sup>41</sup>

All the stationary point has been characterized with real and positive values of vibrational frequency, corresponding to stable minima except for the transition state structure. The transition state has been characterized by only one imaginary frequency (NIMAG=1) referring the first order saddle point on the PES. Intrinsic reaction coordinate (IRC)<sup>42</sup> calculations have also been performed to ascertain the minimum energy pathways (MEP) linking the reactant and product through the transition state on the potential energy surface. The minimum energy path (MEP) is obtained by intrinsic reaction coordinate (IRC) calculation performed using Gonzales-Schelgel steepest descent path in mass-weighted Cartesian with a gradient step-size of 0.01 (amu)<sup>1/2</sup>-Bohr. All the electronic calculations are performed using GAUSSIAN 09 program package.<sup>43</sup>

## **4.3 Results and Discussion**

### **4.3.1 Structural Analysis**

The optimized geometries along with the structural parameters obtained at DFT (B3LYP)/6-311G(d,p)/LanL2DZ level for reactant (R1 and R2), TS1, intermediate (IM1 and IM2), TS2 and Product (P1 and P2) involved in the two steps hydrolysis mechanism of the title complex are shown in Figure 4.2.

*Kinetics and thermochemistry of hydrolysis mechanism of a novel anticancer agent trans-[PtCl<sub>2</sub>(dimethylamine)(isopropylamine)]: A DFT study*

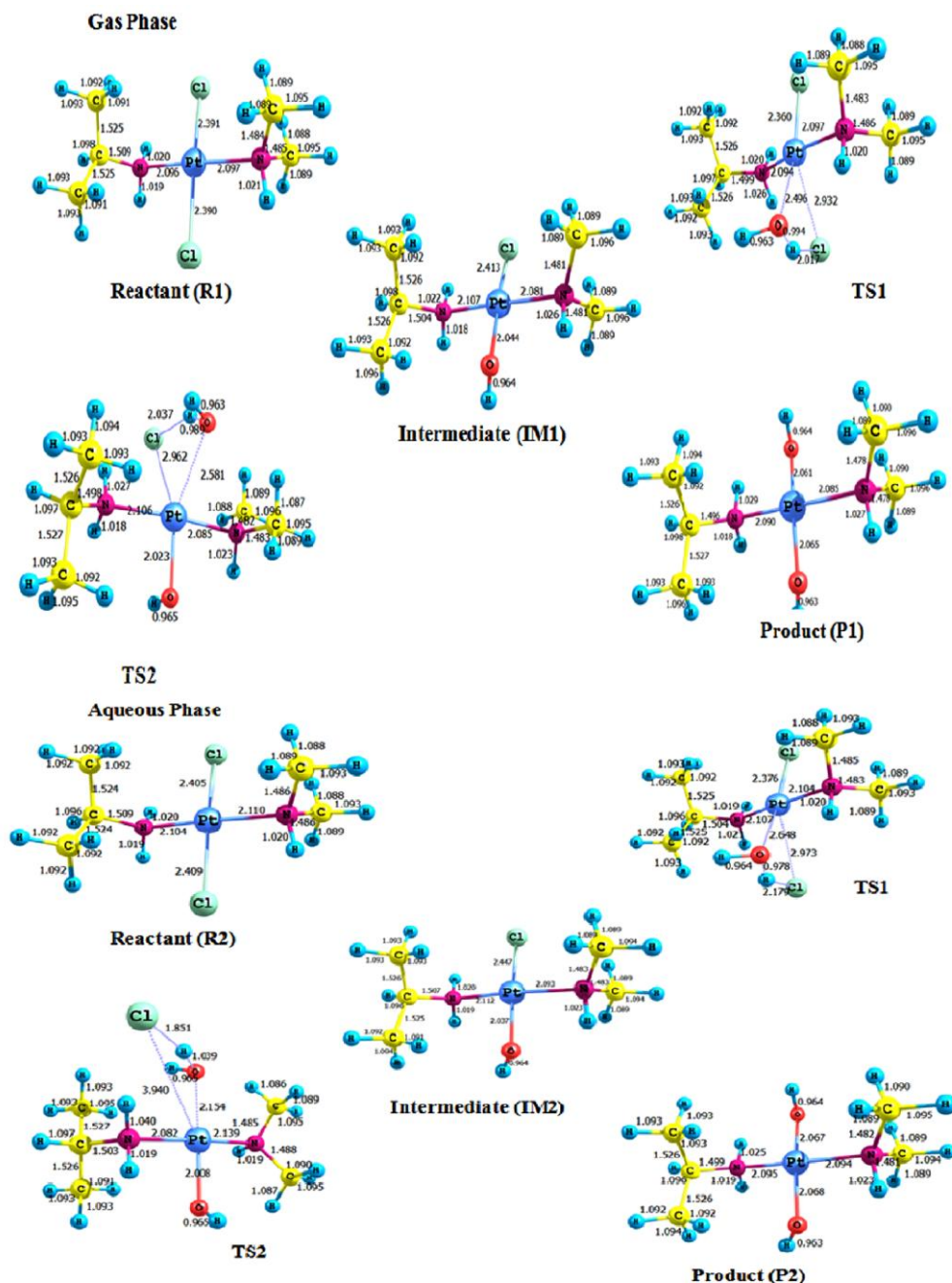


**Figure 4.2** Optimized geometries of the reactant, transition state and product during hydrolysis

The second order nucleophilic substitution ( $S_N2$ ) hydrolysis of *trans*-[PtCl<sub>2</sub>(dimethylamine)(isopropylamine)] is characterized by replacing two Cl<sup>-</sup> ion and followed by the addition of H<sub>2</sub>O molecule. In the first hydrolysis process, one of the *trans*

Cl<sup>-</sup> ion in the complex is replaced by H<sub>2</sub>O, forming the first reaction intermediate (IM1). In the gas phase transition states (TS1), the most important structural changes that have been observed are the breaking of Pt–Cl bond (leaving Cl<sup>-</sup> ion) and formation of the new bond Pt–O (entering H<sub>2</sub>O molecule). From Figure 4.2, in the gas phase, the distance of breaking Pt–Cl bond increases from 2.39 Å in R1 to 2.93 Å in TS1 (almost 23% increase) whereas Pt–O bond distance is observed at 2.49 Å in TS1. At the same time, one of the H-atom of the H<sub>2</sub>O molecule is also coordinating with the leaving Cl<sup>-</sup> ion at a distance 2.07 Å in TS1. In the first intermediate (IM1), one trans Cl<sup>-</sup> ion of the complex is completely replaced by H<sub>2</sub>O molecule (twice). The newly formed Pt–O bond decreases from 2.49 Å in TS1 to 2.04 Å in IM1 (almost 18% decreases). This can be attributed to the more stabilized effect of H<sub>2</sub>O (than Cl<sup>-</sup>) ligand in trans position.<sup>44,45</sup> The intermediate has an almost perfect square planar geometry, with leaving Cl<sup>-</sup> ion completely replaced by H<sub>2</sub>O molecule and formed Pt–OH bond. In the second hydrolysis process, other Cl<sup>-</sup> ion of intermediate is further replaced by H<sub>2</sub>O. During second step, the length of breaking Pt–Cl bond is increased from 2.36 Å in IM1 to 2.96 Å in TS2 (almost 25% increase) whereas Pt–O comes close to 2.58 Å in TS2. The newly formed Pt–O bond decreases from 2.58 Å in TS2 to 2.06 Å in P1 (almost 20% decreases). In this step, the H-atom of H<sub>2</sub>O is also forming a partial bond with the leaving Cl<sup>-</sup> ion at distance 2.03 Å in TS2.

In order to obtain accurate hydrolysis mechanism, the same computational procedure is followed using aqueous phase polarized continuum-model (CPCM). In aqueous phase, the length of the breaking Pt–Cl bond increases from 2.40 Å in IM2 to 2.97 Å in TS1 (almost 24% increase) whereas Pt–O is coming close to 2.64 Å in TS1. The newly formed Pt–O bond decreases from 2.64 Å in TS1 to 2.03 Å in IM2 (almost 23% decreases). In TS1, the H-atom of the H<sub>2</sub>O molecule is coordinating with the leaving Cl<sup>-</sup> ion at a distance 2.17 Å. In the further hydrolysis process, other Cl<sup>-</sup> ion is again replaced by H<sub>2</sub>O molecule. This process is featured by the increase in the Pt–Cl bond from 2.44 Å in IM2 to 3.94 Å in TS2 (almost 61% increase), simultaneously, with a decrease in Pt–O bond from 2.15 Å in TS2 to 2.06 Å in P2 (almost 4% decreases). Here the H atom of H<sub>2</sub>O is forming a partial bond with the leaving Cl<sup>-</sup> ion at distance 1.85 Å in TS2.

### 4.3.2 Energy Profiles

The calculated enthalpy of reaction ( $\Delta_r H^0$ ), reaction free energies ( $\Delta_r G^0$ ) and Gibbs free energy of activation ( $\Delta G^\ddagger$ ) at 298 K for the reaction channels involved in the hydrolysis process are recorded in Table 4.1. Free energy value ( $\Delta_r G^0$ ) and enthalpy of reaction ( $\Delta_r H^0$ ) show that both reaction channels are endothermic. From Table 4.1, it can be clearly visible that the second step hydrolysis is more endothermic compared to the first step for both in gas as well as aqueous phase by a extent of 11.85 kJ mol<sup>-1</sup> and 13.69 kJ mol<sup>-1</sup>, respectively. Thus, from the thermodynamic point of view, the first hydrolysis process may be more favorable compared to the second process.

**Table 4.1** Thermochemical data (kJ mol<sup>-1</sup>) for two steps hydrolysis reaction calculated at DFT (B3LYP)/6-311G(d,p)/Lanl2DZ level of theory

Reaction channels	$\Delta_r H(298)$	$\Delta_r G(298)$	$\Delta G^\ddagger$
<b>Gas Phase</b>			
R+H <sub>2</sub> O →IM+HCl	83.73	85.93	92.71
IM+H <sub>2</sub> O→P+HCl	95.05	97.78	95.43
<b>Solvent Phase</b>			
R+H <sub>2</sub> O →IM+HCl	93.52	96.48	91.73
IM+H <sub>2</sub> O→P+HCl	108.71	110.17	127.80

Frequency calculations are performed in order to ascertain the nature of the species involved in the hydrolysis of the title complex. It has been observed from the frequency calculations that all the species corresponds to the stable minima, having real positive vibrational frequencies on their potential energy surface, except in case of transition state



structure. The transition states (TS1 and TS2) are characterized by only one imaginary frequency observed at  $155i\text{ cm}^{-1}$  and  $169i\text{ cm}^{-1}$  in case of gas phase calculations and  $142i\text{ cm}^{-1}$  and  $45i\text{ cm}^{-1}$  for the TS1 and TS2 in aqueous phase, respectively. Visualization of the imaginary frequency revealed a qualitative confirmation of the existence of transition states connecting reactants and products.

Intrinsic reaction path calculations (IRC)<sup>7</sup> have also been performed for each transition state under same level of theory. The result shows that each transition state smoothly connects the reactant and the product sides. Relative energies (including zero-point correction) for each of the species are determined with respect R+H<sub>2</sub>O and IM+H<sub>2</sub>O and the results are presented in Table 4.2.

**Table 4.2** Zero-point corrected total energy (Hartree) of species involved in hydrolysis reaction in gas and solvent phase calculated at DFT (B3LYP)/6-311G(d,p)/Lanl2DZ level of theory

---

Species	Gas Phase	Solvent Phase
Reactant	-1349.301487	-1349.322386
TS1	-1425.70846	-1425.736428
IM	-964.8688866	-964.8898674
TS2	-1041.275287	-1041.310151
Product	-580.4319577	-580.4515918
H <sub>2</sub> O	-76.42682663	-76.43411848
HCl	-460.8270136	-460.8305407

---

A potential energy diagrams of two step hydrolysis mechanism are constructed with the results obtained at the B3LYP/6-311G(d,p)/Lanl2DZ level and are shown in Figure 4.3. The relative energies calculated using CPCM solvation model in aqueous solution are also indicated in Figure 4.3 (red). In the construction of energy diagram, zero-point energy corrected data as recorded in Table 2 are utilized. These energies are plotted with respect to the ground state energy of R+H<sub>2</sub>O and IM+H<sub>2</sub>O, including ZPE,

which are arbitrarily taken as zero. The barrier height for the first step (TS1) in gas and in the aqueous phase are found to be 52.13 kJ mol<sup>-1</sup> and 52.71 kJ mol<sup>-1</sup>, respectively. For TS2, these barrier heights are found to be 55.91 kJ mol<sup>-1</sup> and 84.55 kJ mol<sup>-1</sup> for gas phase and aqueous phase, respectively. A similar trend has also been observed in most of the platinum bases drugs, so our results are in consistent with the available data.<sup>45-47,18</sup> From the ongoing discussion it is clear that the second step hydrolysis is rate-limiting process, which may be due to the stabilizing effect of the entering H<sub>2</sub>O ligands.<sup>44</sup>

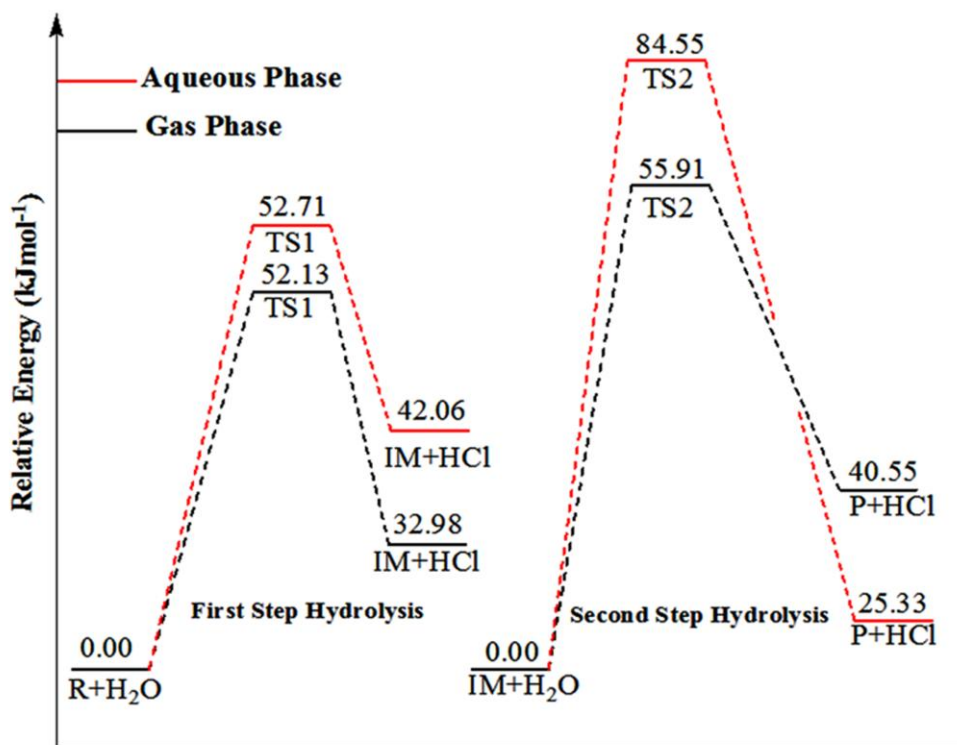


**Figure 4.3** Potential energy surface (PES) of the first and second hydrolysis steps of gas phase (black) and in aqueous phase (red)

The rate constants ( $k$ ) for two steps hydrolysis are calculated with the help of transition state theory. The rate constant expression is given by according to Eyring equation<sup>48</sup>

$$k(T) = \frac{k_B T}{h} e^{-\frac{\Delta G^\ddagger}{RT}} \quad (4.1)$$

where,  $k_B$  is the Boltzmann constant,  $T$  is the absolute temperature and  $h$  is the Planck constant.  $\Delta G^\ddagger$  is the activation free energy for each step.

The rate constant values for the first and second hydrolysis process are computed with the help of the above expression. The values of the rate constant, in gas phase are found to be  $3.67 \times 10^{-4} \text{ s}^{-1}$  and  $1.22 \times 10^{-4} \text{ s}^{-1}$  for the TS1 and TS2, respectively. However, these values in aqueous phase are  $5.44 \times 10^{-4} \text{ s}^{-1}$  and  $2.65 \times 10^{-10} \text{ s}^{-1}$ , respectively. It is clear from the rate constant expressions that first hydrolysis process is somewhat faster compared to that of the second hydrolysis process. These values of rate constant are also in good agreement with the values observed in case of similar types of complexes.<sup>49</sup>

#### **4.4 Conclusion**

In the present manuscript, we have presented a systematic theoretical investigation on the hydrolysis mechanism of the novel anticancer agent *trans*-[PtCl<sub>2</sub>(dimethylamine)(isopropylamine) using DFT. All the structures are optimized along with the vibrational frequency calculations at B3LYP/6-311G(d,p)/Lanl2Dz level of theory in the gas phase as well as in aqueous phase using CPCM model. The hydrolysis is preceded *via* a pentacoordinated trigonal bipyramidal (TBP) transition state structure implying a concerted S<sub>N</sub>2 mechanism. The structures of the transition states (TS1 and TS2) involved in the reaction path are confirmed by using IRC calculations. The activation barrier heights for two step hydrolysis reaction are found to be 52.13 kJ mol<sup>-1</sup> and 55.91 kJ mol<sup>-1</sup> (52.71 kJ mol<sup>-1</sup> and 84.55 kJ mol<sup>-1</sup> for aqueous phase) for the first and second transition state, respectively. Hence, the first hydrolysis step has found to be faster compared to the second step, indicating the monoquo species of the complex is the most preferable species that react with the cellular DNA *in vivo*. From the rate constant studies, it has also been found that the rate constant values for the first step is faster by an extent of  $2.45 \times 10^{-4} \text{ s}^{-1}$  and  $5.43 \times 10^{-4} \text{ s}^{-1}$  in gas phase and aqueous medium, respectively, compared to the second hydrolysis step. The work presented in the manuscript will be very much useful for the further investigation of the reaction mechanism of formation of hydrolyzed complex with its intercellular target DNA. These significantly different rates of the complex are of clinically importance since such differences have unambiguous effect on their anticancer property as well as cytotoxicity.

## References

1. Rosenberg, B. *Cancer* **55** (10), 2303--2316, 1985.
2. Rosenberg, B., et al. *Nature* **222** (5191), 385--386, 1969.
3. Rosenberg, B., et al. *Nature* **205**, 698--699, 1965.
4. Galanski, M., et al. *Curr. Med. Chem.* **12** (18), 2075--2094, 2005.
5. Sherman, S.E., & Lippard, S. *J. Chem. Rev.* **87** (5), 1153--1181, 1987.
6. Brabec, V., & Kasparkova, J. *Drug Resist Updat.* **8** (3), 131--146, 2005.
7. Chabner, B.A., & Roberts, T.G. *Nat. Rev. Cancer* **5**, 65--72, 2005.
8. Kelland, L.R. *Crit. Rev. Oncol. Hematol.* **15** (3), 191--219, 1993.
9. Connors, T. A., et al. *Cancer Treat. Rep.* **63**, 1499--1502, 1979.
10. Cleare, M.J., & Hoeschele, J.D. *Bioinorg. Chem.* **2** (3), 187--210, 1973.
11. Farrell, N. *Transition Metal Complexes as Drugs and Chemotherapeutic Agent*, Kluwer, Dordrecht, The Netherlands, 1989.
12. Natile, G., & Coluccia, M. *Coord. Chem. Rev.* **216-217**, 383--410, 2001.
13. Farrell, N. *Met. Ions Biol. Syst.* **32**, 603--639, 1996.
14. Natile, G., & Coluccia, M. A. Antitumor active trans-platinum compounds, in *Metal Ions in Biological Systems*, H. Sigel et al, eds., Marcel Dekker Inc., New York, Basel, 2004, 209--25.
15. Farrell, N., et al. *J. Med. Chem.* **32** (10), 2240--2241, 1989.
16. Banerjee, S., et al. *Chem. Phys. Lett.* **497** (1-3), 142--148, 2010.
17. Banerjee, S., et al. *Chem. Phys. Lett.* **487** (1-3) 108-115, 2010.
18. Miller, S.E., et al. *Inorg. Chim. Acta* **190** (1), 135--144, 1991.
19. Miller, S.E., & House, D.A. *Inorg. Chim. Acta* **166** (2), 189--197, 1989.
20. Legendre, F., et al. *Chem. Eur. J* **6** (11), 2002--2010, 2000.
21. Raber, J., et al. *Mol. Phys.* **102** (23-24), 2537--2544, 2004.
22. Arnesano, F., & Natile, G. *Coord. Chem. Rev.* **253**, 2070--2081, 2009.
23. Raber, J., et al. *J. Phys. Chem. B* **109** (24), 12195--12205, 2005.
24. Kozelka, J. *Inorg. Chim. Acta* **362** (3), 651--668, 2009.
25. Lau, J.K.C., & Deubel, D.V. *J. Chem. Theory Comput.* **2** (1), 103--106, 2006.
26. Alberto, M.E., et al. *J. Phys. Chem. B* **113** (43), 14473--14479, 2009.

27. Pavelka, M., et al. *Chem. Eur. J.* **13** (36), 10108--10116, 2007.
28. Lucas, M.F., et al. *J. Phys. Chem. B* **113** (3), 831--838, 2009.
29. Lippert, B. (ed.). *Cisplatin: chemistry and biochemistry of a leading anticancer drug*, Wiley-VCH, Zurich, 1999.
30. Eastman, A., et al. *Chem. Biol. Interact.* **67** (1-2), 71--80, 1988.
31. Strandberg, M.C., et al. *Chem. Biol. Interact.* **39** (2), 168--180, 1982.
32. Montero, EI., et al. *J. Med. Chem.* **42** (20), 4264--4268, 1999.
33. Pe´rez, J.M., et al. *J. Med. Chem.* **43** (12), 2411--2418, 2000.
34. Kim, K., & Jordan, K.D. *J. Phys. Chem.* **98** (40), 10089--10094, 1994.
35. Stephens, P.J., et al. *J. Phys. Chem.* **98** (45), 11623--11627, 1994.
36. Raghavachari, K., & Trucks, G.W. *J. Chem. Phys.* **91**, 1062--1065, 1989.
37. Hay, P.J., & Wadt, W.R. *J. Chem. Phys.* **82**, 270--283, 1985.
38. Barone, V., & Cossi, M. *J. Phys. Chem. A* **102** (11), 1995--2001, 1998.
39. Cossi, M., et al. *J. Comput. Chem.* **24** (6), 669--681, 2003.
40. Tílvez, E., et al. *Inorg. Chem.* **54** (4), 1223--1231, 2015.
41. Ritacco, I., et al. *Inorg. Chem.* **55** (4), 1580--1586, 2016.
42. Gonzalez, C., & Schlegel, H.B. *J. Chem. Phys.* **90** (4), 2154--2161, 1989.
43. M.J. Frisch et al. Gaussian 09, Revision B.01, Gaussian, Inc., Wallingford, CT, 2010.
44. McGowan, G., et al. *Inorg. Chem.* **44** (21), 7459--7467, 2005.
45. Lippert, B. Trans-diammineplatinum(II): what makes it different from cis-DDP? Coordination chemistry of a neglected relative of cisplatin and its interaction with nucleic acids, in *Metal Ions in Biological Systems*, H. Sigel et al, eds., Marcel Dekker Inc., New York, Basel, 1996, 209--25.
46. McGowan, G., et al. *Chem. Eur. J.* **11** (15), 4396--4404, 2005.
47. Alberto, M.E., et al. *Inorg. Chem.* **50** (15), 6965--6971, 2011.
48. Conors, K.A. *Chemical Kinetics – The Study of Reaction Rate in Solution*, Wiley, New York, 1990.
49. Alberto, M.E., & Russo, N. *Chem. Commun.* **46**, 5894--5896, 2011.